

# DISCOMFORT GLARE INDEX FOR AUTOMATED BLIND CONTROL

Toshie Iwata<sup>1</sup>, Kensuke Nagayoshi<sup>2</sup>, Werner Osterhaus<sup>3</sup>

<sup>1</sup> Tokai University, Tokyo (Japan)

<sup>2</sup> Kume Sekkei Co.,Ltd, Tokyo (Japan)

<sup>3</sup> Aarhus School of Engineering, Aarhus, (Denmark)

## 1. Introduction

### 1.1. Background

Since using daylight in buildings is expected to be part of the solution for global warming, controlling the amount of light and heat is important. Venetian blinds are the most-widely-used shading system in office spaces. Automated blinds control systems which are admissible for the Comprehensive Assessment System for Built Environment Efficiency (CASEBEE, 2008) point system, have been widely used in office buildings in Japan. Compared with offices in European countries, there are two significant reasons why automated blind control is required for offices in Japan. The first one is the climatic condition and the second is the type of office, which is typically “open-plan”.

Japan belongs to the temperate zone with four distinct seasons, but its climate varies from cool temperate in the north to subtropical in the south. Central Japan has hot, humid summers and short winters. A simulation study using climate data was carried out to show the difference in annual air conditioning load for a model office building in Tokyo and in five European cities: Rome, Zurich, Paris, Frankfurt and London (Roh and Udagawa, 2002). It is shown that the annual space cooling load is much greater than the space heating load in all cities, because the space cooling load of office buildings is affected by solar radiation through windows and internal heat gains. Although, in the European cities, the cooling effect of the fresh air introduced as ventilation requirement contributes to reduce the cooling coil load of air handling unit, such effect cannot be expected in Tokyo. Controlling solar radiation through windows is usually the most effective strategy for energy savings in Tokyo

Open-plan offices are so common in Japan that it is difficult to find private office spaces. Surveys of 779 open-plan-office occupants in five large Canadian and US cities showed that open-plan office occupants who were more satisfied with their environments were also more satisfied with their jobs. It was suggested that the physical environment has a role in organizational well-being and effectiveness (Veitch et al., 2007).

In common automated blind control systems, the blind status (slat and blind up/down position) depends on the daylight information obtained via rooftop measurement and calculated solar position. The amount of light from dimmable electric lighting which is determined by occupancy sensor and illuminance on the desk has effects on the heating/cooling load. The control system can significantly reduce energy for lighting and cooling.

### 1.2. Purpose

In the early stage of automated blind control, the operation was often changed from automatic control to manual control by workers who had not been satisfied (Iwata and Tokura, 2002). It was learned that the blind slat angle should be decided not only to cut direct sunlight but also to prevent discomfort glare. To evaluate discomfort glare from daylight, there are evaluation methods using images of luminance distribution, whose validity has been examined (Iwata and Osterhaus, 2010). However, it is difficult to apply these glare evaluation methods to automated control blind in an open-plan office, which has large windows as well as a large floor area. Apart from the basic problem of calculation of glare indices, e.g. the determination of glare source and background, there are problems, e.g. the distribution of the workers' desks (observation points), the view directions and zoning of the blinds. The purpose of this paper is to address these problems in applying the existing evaluation methods to automated blind control.

## 2. Glare indices for daylight and blind control

### 2.1. Glare indices for daylight

The cause of the sensation of discomfort glare appears to be a compounds of two effects. One is a contrast effect and the other is a saturation effect. The contrast effect is dominant for small glare sources, while the contrast effect is considered smaller and the saturation effect should be taken into account for large sources.

For daylight glare, several evaluation methods using images of luminance distribution have been developed. These include Daylight Glare Probability (DGP) (Wienold and Christoffersen, 2006), Predicted Glare Sensation Vote (PGSV) (Iwata et al., 2008), the statistical value-based indicators  $L_{\text{mean}} / L_{\text{median}}$  (ratio between mean and median values of luminance) (Osterhaus, 2008) and the “discomfort glare image developed from brightness image” method (Sugano and Nakamura, 2011).

DGP, which shows the probability of persons being affected by discomfort glare, is defined by the following equation.

$$DGP = C_1 E_v + C_2 \log \left( 1 + \sum \frac{L_{si}^2 \omega_{si}}{E_v^{c_4} P_i^2} \right) + C_3 \quad (\text{Eq.1})$$

$$C_1 = 5.87 \times 10^{-5} \quad C_2 = 9.18 \times 10^{-2} \quad C_3 = 0.16 \quad C_4 = 1.87$$

where  $E_v$  is the vertical eye illuminance [lx],  $L_s$  is the luminance of source [ $\text{cd m}^{-2}$ ],  $\omega$  is the solid angle of source [sr] and  $P$  as the Position Index.

The first term indicates the saturation effect while the second term indicates the contrast effect. To calculate the second term, the threshold luminance which determines whether a particular light source in the field of view is to be considered a glare source, rather than being part of the background should be decided. In DGP a luminance four times higher than the adaptation luminance was selected as the threshold luminance.

PGSV, which shows the glare sensation (0: just perceptible to 3: just intolerable), is defined by the following equations:

when  $L_s/L_b > L_{ave}/L_{ad}$  (contrast glare)

$$PGSV_{cont} = \log \frac{L_s^{c_1} \omega^{c_2}}{L_b^{(c_3 - c_4 \log \omega)}} - C_5 \quad (\text{Eq.2})$$

$$C_1 = 3.2 \quad C_2 = -0.64 \quad C_3 = 0.61 \quad C_4 = 0.79 \quad C_5 = -8.2$$

when  $L_s/L_b \leq L_{ave}/L_{ad}$  (saturation glare)

$$PGSV_{sat} = \frac{-A_1 - A_2}{1 + (L_{ave}/L_0)^{P_1}} + A_2 \quad (\text{Eq.3})$$

$$A_1 = -0.57 \quad A_2 = -3.3 \quad L_0 = 1270 \quad P_1 = 1.7$$

where  $L_b$  is the background luminance [ $\text{cd m}^{-2}$ ],  $L_s$  is the luminance of the source [ $\text{cd m}^{-2}$ ],  $L_{ave}$  is the mean luminance of the visual field ( $L_{ave} = E_v \pi^{-1}$ ),  $L_{ad}$  is the adaptation luminance [ $\text{cd m}^{-2}$ ],  $\omega$  is the solid angle of the source [sr].

To calculate  $PGSV_{cont}$ , there are two methods. In the first method, the threshold luminance between source and background is determined by finding the luminance which produces the highest ratio of the mean source luminance to the mean background luminance. In the second method, which is simpler than the first method, the whole window area is considered as a glare source, in advance. Our previous paper shows that the simpler method (the source-fixed method) can be used when the blind reflectance is not extremely low (Iwata et al., 2011).

The ratio of mean luminance to median luminance ( $L_{\text{mean}} / L_{\text{median}}$ ) proposed by Osterhaus (2008) is based on the fact that the mean value, rather than the median value, is influenced by extreme (higher/lower) values outside the normal distribution. The larger the ratio of mean luminance to median luminance becomes, the greater the likely glare perception.

Sugano and Nakamura (2011) proposed a method of calculating discomfort glare images from brightness images, in which luminance distributions were converted by using a wavelet transform. This method can predict discomfort glare from each point in the visual field when an observer looks at the point.

In our previous papers (Iwata and Osterhaus, 2010) (Iwata et al. 2011), the applicable range of three of such glare indices (DGP, PGSV, and  $L_{\text{mean}}/L_{\text{median}}$ ) were examined and the results show that DGP, which overestimates discomfort glare when DGP is low and underestimates discomfort glare when DGP is high, appears suitable to assess an environment for which the luminance contrast within visual field is small. The  $L_{\text{mean}}/L_{\text{median}}$  method, which appears to be suitable in relative assessment, can predict discomfort from contrast effects. For  $\text{PGSV}_{\text{cont}}$ , it was found that the borderline between the condition for  $\text{PGSV}_{\text{cont}}$  and that for  $\text{PGSV}_{\text{sat}}$  produces a gap in the predicted level of glare.

## *2.2. Practical use of glare evaluation methods in blind control*

In the planning phase of an office building, a glare simulation tool, i.e. a combination of a simulation program calculating luminance distributions and one of those daylight glare evaluation methods, can contribute to designing a façade of the building. Especially time-series simulation using annual climate data is helpful to decide size, position and optical properties of window glazing and shading devices. To conduct hourly or shorter time steps, a reduction of calculation time is required. For DGP, simplified methods were used to calculate the second term of the equation representing the contrast effect (Wienold, 2009; Johnsen, 2008). For PGSV, the simpler (source-fixed) method was used to calculate  $\text{PGSV}_{\text{cont}}$  (Itoh and Iwata, 2007a).

For actually controlling the blind during operation, continuous measurements are required to calculate the predicted glare level with each method to determine the required slat angle of the blind. Measurements of luminance distributions using a CCD camera make it easy to calculate those glare indices. However, in an open-plan office, there are various observation points, so that measurements by CCD camera are not practical.

There are several aspects which disturb these glare evaluation methods that directly apply to automated blind control in open-plan offices: the observation points, the view directions and the zoning of the blinds.

## **3. Flow of automated blind control**

Venetian blinds are commonly used for automated control in office spaces. Figure 1 shows the flow of the existing blind control method based on discomfort glare. The necessity of adjusting the slat angle is judged depending on the amount and the angle of direct sunlight striking the façade. If slat angle control is necessary, the cut-off angle is determined so as to exclude direct sunlight from entering the room. Since the slat angle should be decided not only to cut direct sunlight but also to prevent discomfort glare, a given glare index value is calculated and compared to the glare index limit. If the calculated glare value is not less than the limit, the additional slat angle (off-set angle) is required. Until the glare index value calculated decreases to reach the limit value, this loop continues (Nagayoshi et al., 2011).

Usually, blinds are controlled all together and it is assumed that the position where the most severe glare is experienced is near the façade. Thus this flow is carried out for only one observation point and one zone of the blinds. This conventional method is rather simple, but there is a chance that it closes the blinds more often than necessary.

## **4. Numerical simulations**

### *4.1. Simulation model*

To identify an effective way for controlling blinds in open-plan offices, an office space as shown in Figure 1 is used as a simulation model. It has a glazed south-facing façade with a window sill at 0.7m above the floor. The height of the ceiling is 2.7m

There are rectilinear cubicles created using modular systems furniture as shown in Figure 3. The height of the partition equals eye height, 1.2m, so that the workers cannot see the window below eye height. The workers see the downward side of the blind slat.

There are various observation points, e.g. 3 m (A), 6 m (B), and 12 m (C) from the façade, and blind positions, e.g. blinds I to VI, as shown in Figure 2.

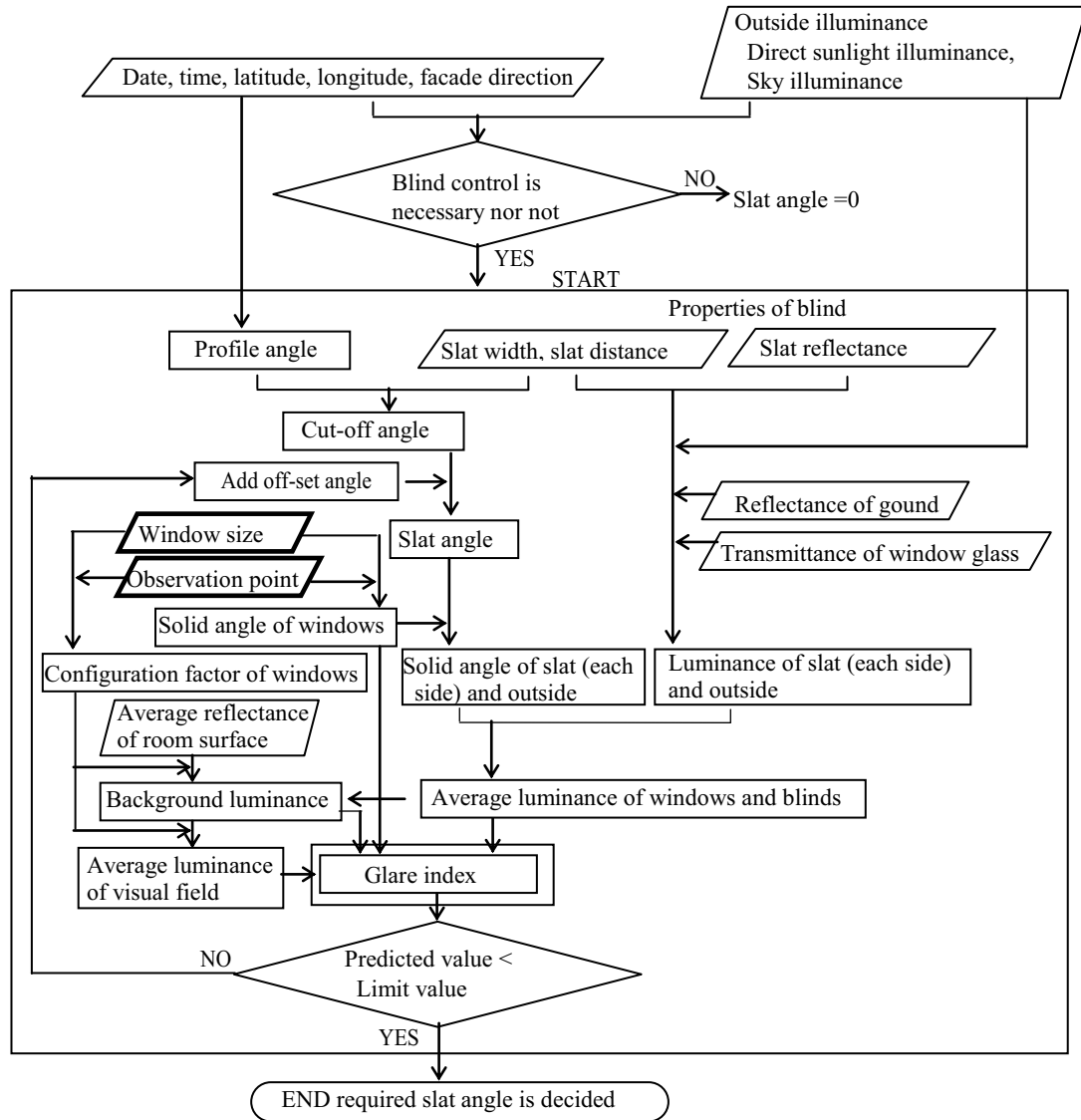


Fig. 1: Control flow of automated blind

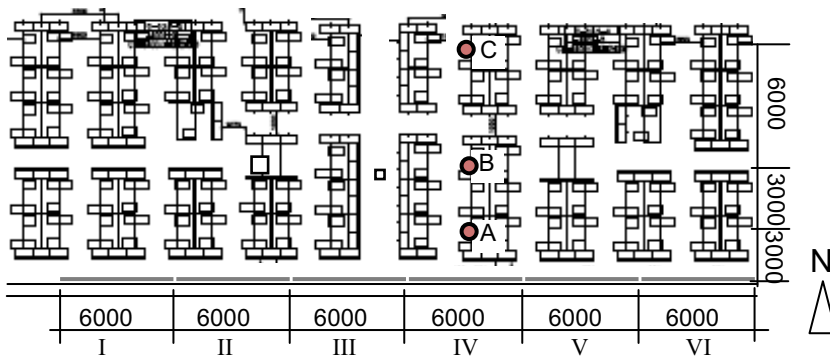


Fig. 2: Plan of open-space office for simulation



Fig. 3: Work station in office space

The slat of the venetian blind is 35 mm in width and the distance between the slats is 30 mm. The color is diffuse white with of 0.8 of reflectance  $\rho_{vis}$ . Lambertian reflection is assumed. They are lowered completely and the default setting of the slat angle is the cut-off position as shown in equation 4.

$$\theta_{suncut} = \text{atan} \left( \frac{\frac{S}{W} \cos \alpha_p}{\sqrt{1 - \left(\frac{S}{W} \cos \alpha_p\right)^2}} \right) - \alpha_p \quad (\text{Eq.4})$$

where  $\theta_{suncut}$  is the cut-off angle,  $\alpha_p$  is the profile angle,  $S$  is the distance between the slats (30 mm), and  $W$  is the slat width (35mm).

The reflectance of the ceiling is 0.8, while the equivalent reflectance of lower surface is 0.1. The glazing's visual transmittance is presented by a function of the incident angle as shown in Figure 4. For diffused light, the incident angle is assumed to be 60 degrees.

Previous research shows the luminance of the blind slat and the luminance of sky, which is seen between the blind slats, as shown in Figure 5 (Itoh and Iwata, 2007b). The ratio of the luminance of the slat to that of the sky ranges from 0.2 to 1, approximately. Therefore in this study, the whole window area, including the blind slats, is considered as glare source.

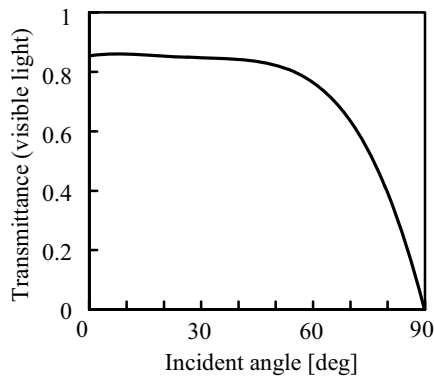


Fig. 4: Transmittance of window glass

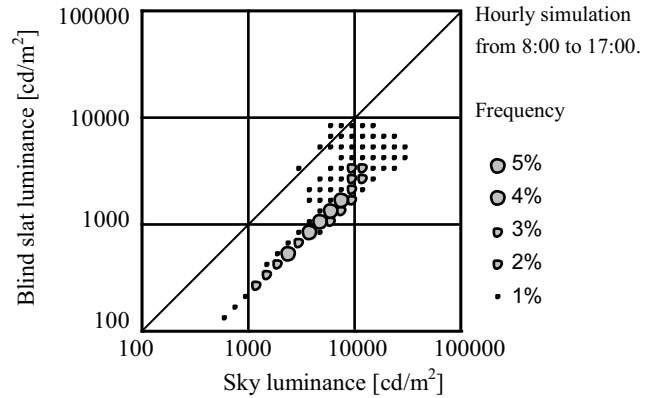


Fig. 5: Sky luminance and luminance of blind slat  
Weather data is Tokyo standard year provided by the Expanded AMeDAS weather data. Blind slat is at cut-off angle position, when the sky index  $S_i$  (Igawa et. al., 2004) is larger than 3.

## 4.2. Preliminary examinations

### 4.2.1. Range of solid angle of sources

In open-plan offices, blinds are usually controlled all together (as-one control). However, workers are not always working at their desks. In order to examine the possibility of multi-zone control, the maximum solid angle of the source which has an effect on contrast glare and saturation glare is calculated.

It is known that the larger the horizontal displacement of the source from the observer's line of sight, the larger the luminance required to cause the same glare sensation. The position index expresses the change in discomfort glare experienced relative to the angular displacement (azimuth and elevation) of the source from the observer's line of sight.

Guth's Position Index (P) was calculated by using the equation proposed by the IES (Eq. 5) for the visual field above the line of sight (IES, 1984).

$$\ln P = (35.2 - 0.31889\gamma - 1.22 \exp(-2\gamma/9)) \times 10^{-3} \sigma + (21 + 0.26667\gamma - 0.002963\gamma^2) \times 10^{-5} \sigma^2 \quad (\text{Eq.5})$$

where  $\gamma$  is the  $\tan^{-1}(x/y)$  (deg),  $x$  and  $y$  are the horizontal and vertical distance (m) between the point of view and the source respectively, and  $\sigma$  is the angle between the line of sight and line from the observer to the source (deg).

When Hopkins developed the Daylight Glare Index (Cornell formula), he proposed a “modified solid angle”, which is the solid angle of the source modified by the position of the source. The modified solid angle is defined by the following equation (Hopkinson and Bradley, 1960).

$$\Omega = \sum \frac{\omega_{si}}{P_i^2} \quad (\text{Eq.6})$$

where  $\omega_{si}$  is the solid angle of source [sr] and  $P_i$  as the Position Index.

In the second term of DGP, which presents the contrast effect, the same concept as the modified solid angle is shown (see Equation 1).

Figure 6 illustrates the relationship between the horizontal angle of the window and the solid angle, the configuration factor and the modified solid angle of the window, for the case shown in Figure 7. The configuration factor is calculated for the eye plane. When the horizontal angle is more than 90 degrees, the increments of the configuration factor and the modified solid angle, which are parameters of DGP, are diminished. The solid angle, which is one of parameters of PGSV, increases even when the horizontal angle of the window is larger than 90 degrees.

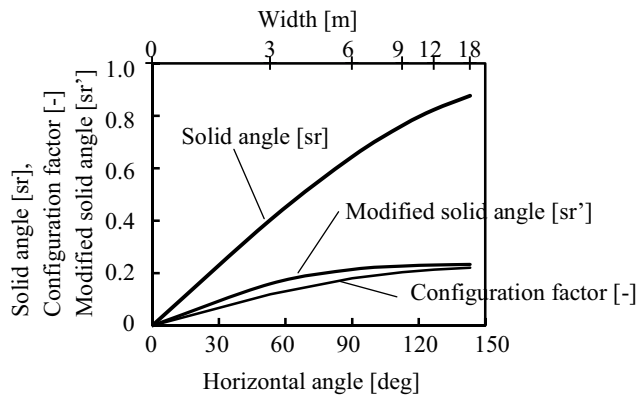


Fig. 6: Horizontal angle of window and solid angle, configuration factor and modified solid angle of window

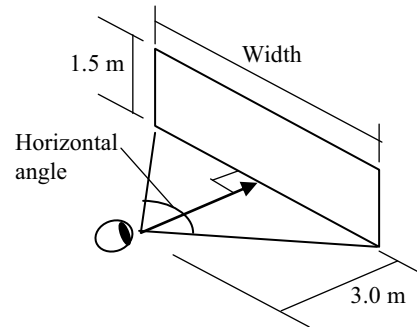


Fig. 7: Horizontal angle and width of window and view point

Figure 8 shows the solid angle of the window for different distances between the façade and the observation points. Since the height of the window is not changed, the shorter the distance, the larger the solid angle. To compare the change in solid angle calculated for each distance, the solid angle is converted into the relative solid angle as shown in Figure 9, in which the ratio of solid angle for each horizontal angle to that for 90 degrees of the horizontal angle is used in the Y-axis. The ratio remains constant for 90 degree horizontal angles.

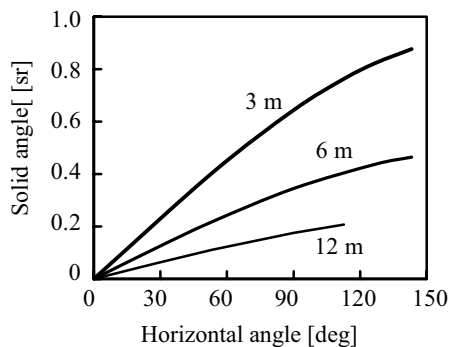


Fig.8: Horizontal angle vs. solid angle for different distance between façade and observation point

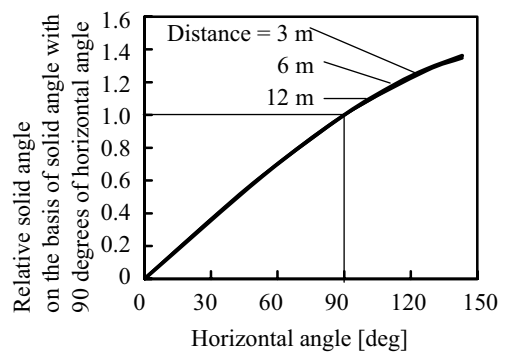


Fig. 9: Horizontal angle vs. relative solid angle for different distance between façade and observation point

Figure 10 shows the change in the configuration factor and the modified solid angle of the window. The modified solid angle seems to reach the maximum value. The configuration factor increases even when the horizontal angle is larger than 120 degrees. In DGP, the modified solid angle is used to evaluate the contrast effect, while the configuration factor is used to calculate the vertical illuminance at the eye plane (saturation effect).

#### 4.2.2. Effect of distance between façade and observation point

As mentioned in 4.2.1, when the distance between the façade and the observation point increases, the solid angle, the configuration factor and the modified solid angle of the window decrease. However, the ratio of the solid angle of outside view, which can be seen between the slats, to the solid angle of the window increases with the distance between the façade and the observation point as shown in Figure 11. If the outside view mainly consists of sky with a high luminance, the average luminance of the window area increases with the distance between the façade and the observation point.

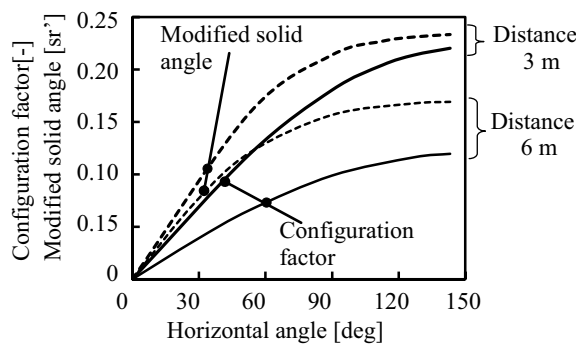


Fig. 10: Horizontal angle of window vs. configuration factor and modified solid angle of window

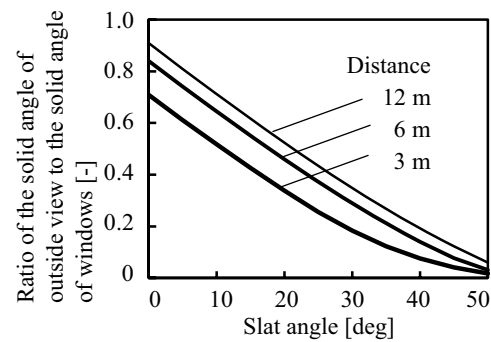


Fig. 11: Slat angle vs. ratio of outside view to window area (under assumption that slat thickness is negligible)

#### 4.2.3. Effect of viewing direction

Usually workers are seated parallel to the window. The effect of view direction on the solid angle, the configuration factor and the modified solid angle of the window were examined for two cases. In the first case, the observation point is changed, while in the second case the line of sight of an observer is changed. Figures 12 and 13 show the first and the second cases, respectively. The Y-axis shows the relative value for each view angle to the value for the view angle of 0 degrees (perpendicular to the façade).

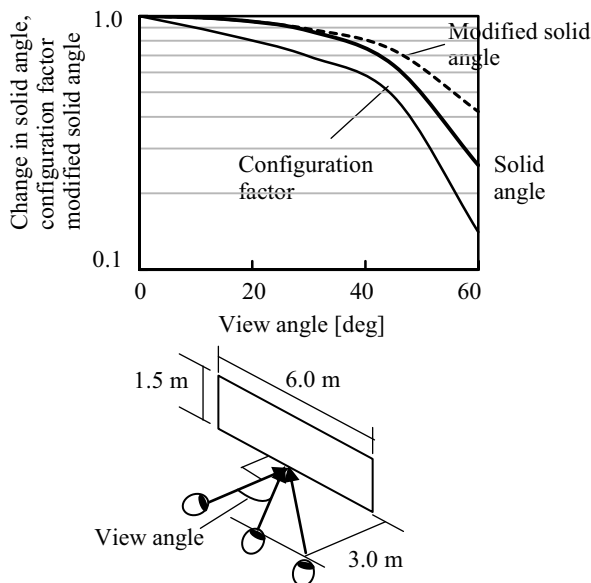


Fig. 12: Effect of view direction on solid angle, configuration factor and modified solid angle of window (case 1)  
When view angle = 0, each value =1

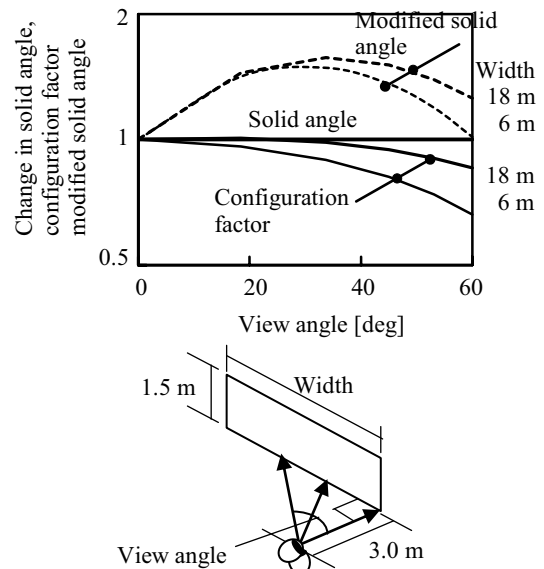


Fig. 13: Effect of view direction on solid angle, configuration factor and modified solid angle of window (case 2)  
When view angle = 0, each value =1

In the first case the solid angle, the configuration factor and the modified solid angle of the window decreases with increasing view angle. In the second case, the solid angle shows a constant value. As shown in Figure 12, the modified solid angle increases with view angle until it reaches a peak value, while the configuration factor continuously decreases.

The effect of view direction on the ratio of outside view is also examined. The effect is so small that the difference cannot be identified on a figure illustrating the relationship between the ratio of the solid angle of outside view seen between the slats to the solid angle of the windows. It is thus sufficient to calculate it for only one view.

#### 4.2.4. Effect of outside view

It is reported that a view with a great deal of interesting information extends subjects' tolerance level of discomfort glare (Tuaycharoen and Tregenza, 2005, Yun et al., 2010). Apart from "interesting information from the outside view", the luminance of the view elements is an important factor for evaluating glare from windows. Since outside objects e.g. walls or roofs of buildings, trees, usually have a lower luminance than the sky, the ratio of the apparent size of these objects to that of the sky should be calculated. This ratio usually increases with the increment of the distance between the façade and the observation point. This fact should be taken into account to when calculating glare indices from various observation points.

### 4.3. Simulation on the slat angle and glare indices

#### 4.3.1. Effect of source size assumed as a glare source on Glare indices

Figures 14 and 15 show the difference in DGP and PGSV between two different calculation methods. The first one considers a window width of 30 m (horizontal window angle = 157 degrees, solid angle = 0.91 sr) as a glare source, while the second one considers a width of 6 m (horizontal window angle = 90 degrees, solid angle = 0.64 sr) as a glare source. Simulation conditions are as follows: latitude 35.3°N (Tokyo), noon solar time at equinox, 60 klx of horizontal illuminance from direct sunlight and 25 klx of horizontal sky illuminance. In this condition, the cut-off angle is 0 deg.

DGP shows approximately the same value, because the difference in the modified solid angle and the configuration factor of the window between 90 degrees and 150 degrees of the horizontal angle of the window is small as shown in Figures 5 and 9. Also PGSV shows small difference, because smaller solid angle of the 90 degree-width window is compensated by its larger background luminance.  $L_{\text{mean}}/L_{\text{median}}$  is independent from the solid angle of the area assumed as the source.

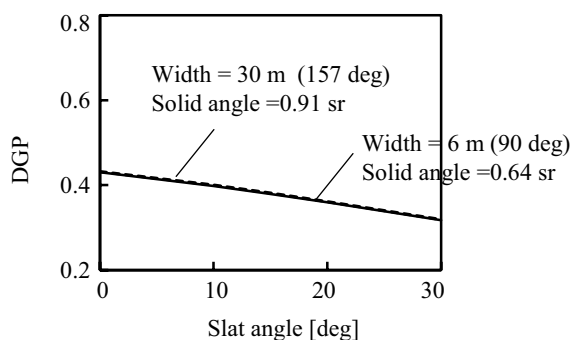


Fig. 14: Effect of width of window assumed as a glare source on DGP

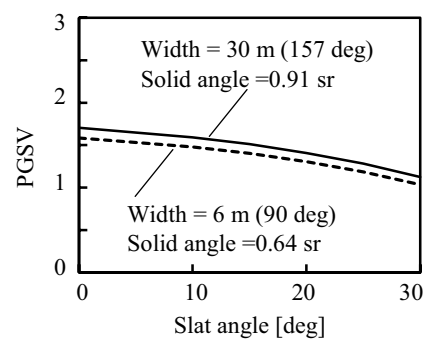


Fig. 15: Effect of width of window assumed as a glare source on PGSV

#### 4.3.2 Effect of control zone

In order to examine the possibility of control for each zone ("each-zone" control), glare indices for each-zone control and "as-one" control were calculated. For the each-zone control, it is assumed that the width of controlled blind is 6 m and that the line of sight is perpendicular to the façade. For the observation point A, the slat angle of the blind zone IV is changed (see Figure 2), while the slat angles of the other blinds are kept at 0 degree (horizontal position). The other conditions are the same as in the previous section. Figures 16, 17 and 18 show the difference between "each-zone" control and "as-one" control.



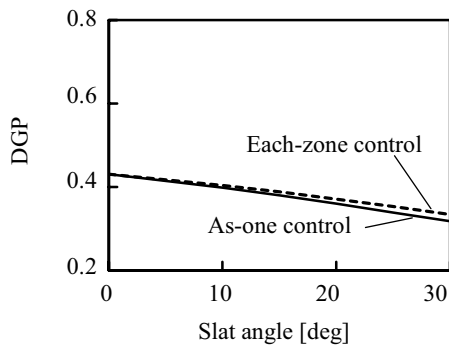


Fig. 16: Effect of blind control zone on DGP

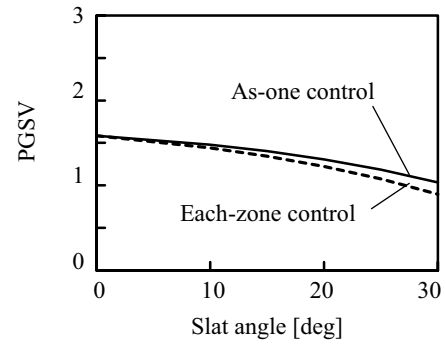


Fig. 17: Effect of blind control zone on PGSV

The each-zone control shows a higher DGP and  $L_{\text{mean}}/L_{\text{median}}$  than the as-one control, when the slat angle is larger. However, the difference is very small. On the other hand, the each-zone control shows a lower PGSV than the as-one control when the slat angle is larger. The difference is also very small. Compared with the each-zone control, the as-one control, which reduces the vertical illuminance at the eye plane  $E_v$ , reduces DGP and  $L_{\text{mean}}$ . For PGSV, reducing  $E_v$  means increasing the background illuminance. Other seasons are tested and they show a similar tendency. Therefore, it can be said that these glare indices show the possibility of the each-zone control.

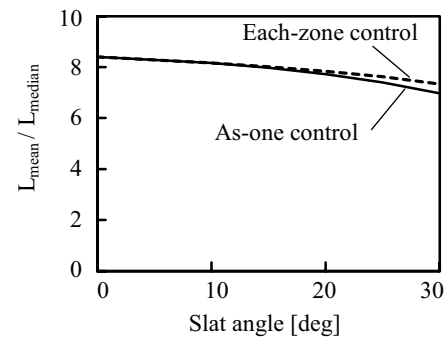


Fig. 18: Effect of blind control zone on  $L_{\text{mean}}/L_{\text{median}}$  is considered that  $L_{\text{mean}}$  is equal to  $E_v/\pi$  and that  $L_{\text{median}}$  is equal to ceiling luminance.

#### 4.3.3 Effect of viewing direction

The effect of view direction on DGP and PGSV is examined. Figures 19 and 20 show the results in the case shown in Figure 12, where the line of sight of an observer is changed. DGP shows small difference between 0 and 45 degrees of view angles, because the larger solid angle of 45 degrees of view angle is compensated by its smaller configuration factor. Both view angles show a rather small DGP. For PGSV, a 45-degree view angle shows a higher value than a 0-degree view angle by 0.15.

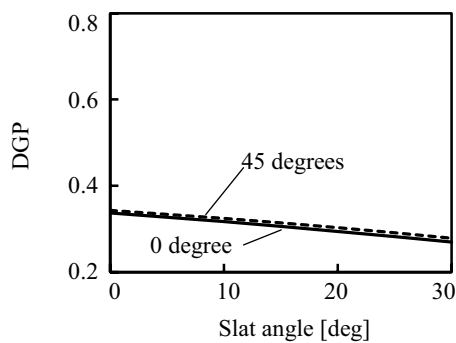


Fig. 19: Effect of view direction on DGP

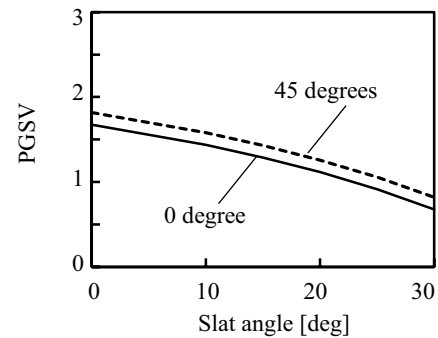


Fig. 20: Effect of view direction on PGSV

#### 4.3.4 Effect of distance from the façade and slat angle

When the blind slat angle increases, the average window luminance decreases. There are two reasons for this. One is that luminance of the slat is decreased because the larger the slat angle, the smaller the form factor between two slats (downward surface of the upper slat and upward surface of the lower slat). The other reason is that the ratio of the solid angle of outside view seen between the slats to the solid angle of window is decreased. A high vertical illuminance on the window plane from direct sunlight results in a high luminance of the blind slat. Therefore, in this case, it is important to reduce slat luminance. When the sky illuminance is high, the solid angle of the outside view should be reduced. Thus, depending on the weather conditions, ways for reducing the average window luminance vary. In this section, weather data for typical

clear days in summer (August 10) and in winter (January 10) in Tokyo are used. At noon on a clear summer day, the horizontal direct sunlight illuminance is 80 klx, while the sky illuminance is 30 klx. The solar altitude is 70.5 degrees. On a clear winter day, the horizontal direct illuminance is 40 klx, while the sky illuminance is 13 klx. The solar altitude is 32.5 degrees.

Figures 20 and 21 show the difference in the effect of slat angle on DGP and PGSV for two positions and seasons. For a clear winter day, a sun-cut-off angle of 13.8 degrees is necessary, so that more than 13.8 degrees of slat angle is shown.

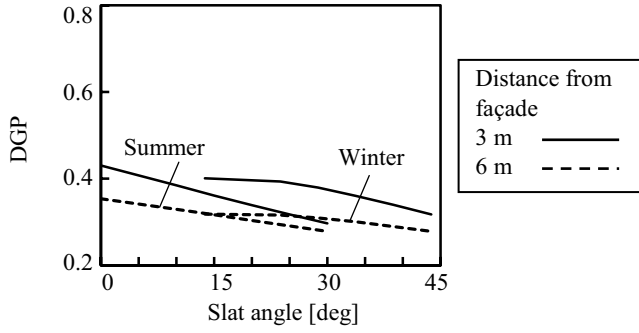


Fig. 21: Effect of season and distance between façade and observation point on DGP

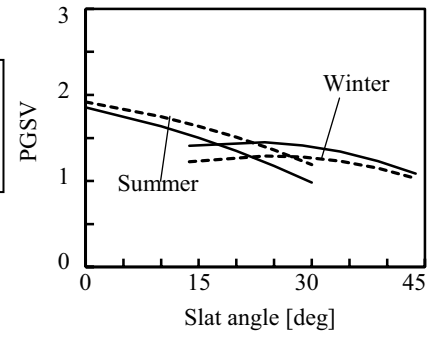


Fig. 22: Effect of season and distance between façade and observation point on PGSV

For DGP, the effect of the distance between the façade and the observation point is obvious. DGP for the shorter distance shows a higher value. It is caused by the fact that a shorter distance causes a higher vertical illuminance at the eye plane. The limit value of DGP for ‘best class’ is 0.35 and for ‘good class’ is 0.4, (Wienold 2009). To achieve a ‘good class’ rating at 3 m from the façade, the cut-off angle is not sufficient either on a clear summer day nor on a clear winter day. To achieve a ‘best class’ rating, an off-set angle of 15 to 20 degrees is necessary on summer clear day and 20 to 25 degrees of off-set angle on winter clear day. Wienold’s study (2009) shows that the cut-off angle plus 20 degrees of blind slat angle can keep a DGP rating of less than 0.35 for 95% of working hours. It can be considered that our results agree with Wienold’s results, because the difference in profile angle between Tokyo and Freiburg can be eliminated by using the cut-off angle.

On the other hand, the observation point at 6m from the façade shows higher PGSV than the observation point at 3m on a clear summer day, while it shows a lower PGSV on a clear winter day. This is caused by the difference in the sky luminance between the summer day and the winter day. On a clear summer day, an off-set angle of 25 to 30 degrees is required to achieve an 80% worker satisfaction 6m from the façade. On a clear winter day, an off-set angle of 25 to 30 degrees is required to achieve an 80% worker satisfaction 3m from the façade.

There are differences in the concept of “glare limit value” (acceptable range) between DGP and PGSV. For DGP, a ‘best class’ rating, where the DGP limit is 0.35 or less, means that the perceived glare is ‘imperceptible’ for 95% of working hours. For PGSV, a Glare Sensation value is converted into “acceptability in an office” based on the results of subjective experiments (Iwata and Osterhaus, 2009). In this method 80% of acceptability means that 80% of workers working at the position do not object to the glare experienced. Therefore, the acceptability in the space is calculated as

$$Ac_{space} = \frac{\sum Ac_i n_i}{\sum n_i} \quad (\text{Eq.7})$$

where  $Ac_{space}$  is the acceptability in the space,  $Ac_i$  is the acceptability of each position,  $n_i$  is the number of workers at the position where the same degree of glare is experienced.

The annual acceptability for each worker is calculated as

$$Ac_{year} = \frac{\sum Ac_i t_i}{\sum t_i} \quad (\text{Eq.8})$$

where  $Ac_{year}$  is the acceptability for a year of a worker,  $Ac_i$  is the acceptability of each time,  $t_i$  is the hour when the same degree of glare is experienced.

On a clear winter day, the effect of the slat angle on both DGP and PGSV is small until the slat angle reaches 30 degrees. On a clear winter day, the vertical illuminance from direct sunlight is high due to a low solar altitude, so that the luminance of a slat is higher than the sky luminance.

## 5. Subjective evaluation and line of sight

### 5.1. Methods

Field experiments with actual windows and venetian blinds were carried out. The test room had windows facing south. Discomfort glare from these windows was evaluated with three different blind slat angle conditions. The three slat angle conditions were the cut-off angle (which prevented direct sun reaching the work space), and two further slat angles which tilted the blinds beyond the cut-off angle by an additional 15 or 20 degrees, respectively.

They were evaluated from two positions, 2.5 m and 5.4 m from the facade. The solid angles of the window were 0.85 sr and 0.34 sr respectively for the two positions. The changes in direction of the line of sight of each subject was measured by an eye-mark recorder (NAC EMR-9).

### 5.2. Results

The results show that the highest glare is observed when the observer's line of sight is perpendicular to the window plane, except around sunset time. It is also shown that higher glare is observed from the position near the façade. Subjects tend to move their view direction frequently when viewing a window, resulting in changing glare experiences. The detailed results of these eye movements are still under analysis.

## 6. Conclusions

In order to apply the existing glare evaluation methods to automated blind control in an open-plan office with a large window, numerical simulations and a subjective experiment were carried out and the following conclusions obtained:

1. When the horizontal angle of a window is larger than 90 degrees, the effect of the increment of the source size on the value of both DGP and PGSV is small.
2. The highest glare is observed when the observer's line of sight is perpendicular to the window plane.
3. "Each-zone" control can be applied when the difference in the slat angle is less than 30degrees.
4. Different seasons and positions relative to the window require different slat angle settings.
5. On a clear day, the cut-off angle is insufficient to result in acceptable DGP or PGSV ratings. DGP and PGSV suggest that an additional off-set angle between 15 and 30 degrees is required.
6. When the vertical illuminance from direct sunlight is large and the sky luminance is rather low, the effect of the slat angle on both DGP and PGSV is small until the slat angle reaches 30 degrees.

## 7. Acknowledgements

This work is supported by a KAKENHI Grant-in-Aid for Scientific Research (B) (No.21360281). The basic idea of this paper is developed from a part of research project of Obayashi Corporation and Tokai University.

## 8. References

- CASBEE for New Construction, 2008.
- Hopkinson, R.G. and Bradley, R.C., 1960. A study of glare from very large sources, *Illuminating Engineering*, Vol. 55, 288-294.
- IES Lighting Handbook, 1984. Reference Volume, *Illuminating Engineering*, Society of North America, pp. 9-46, 9-49.
- Igawa, N., Koga, Y, Matsusawa, T, and Nakamura, H., 2004. Models of Sky radiance distribution and sky luminance distribution, *Solar Energy*, 77, 137-157.
- Itoh. D. and Iwata, T., 2007. Study on automated blind control based on visual comfort , Proc. of 26<sup>th</sup> CIE session, D3, 22-25.
- Itoh. D. and Iwata, T., 2007. The effect of the ratio of blind slats luminance to outside luminance on occupants' satisfaction with a view through blinds, *J. of Environmental Engineering*, Architectural Institute of Japan No. 622, 17-23.
- Iwata T. and Osterhaus W., 2010. Assessment of discomfort glare in daylit offices using luminance distribution images, Proc. of CIE Conference Lighting Quality & Energy Efficiency, 174-180.
- Iwata T., Osterhaus W. and Itoh, H., 2011. Assessment of discomfort glare from windows with venetian blinds using luminance distribution images, Proc. of 27<sup>th</sup> CIE session, Vol.1, 751-757.
- Iwata T. and Tokura M., 2002. Survey on workers' response to automated blinds and lighting control systems in an office, IEA Task 31 and CIE Division 3 mini-conference.
- Iwata, T., Sasaki, M., Mochizuki, E., Itoh, D. 2008. Evaluation of contrast glare and saturation glare by using average luminance of the visual field, Proc. of Balkan Light, 141-146.
- Johnsen, K., 2008. Practical use of new visual discomfort probability index in the control strategy for solar shading devices, Proc. of Indoor Air 2008, paper ID 457.
- Nagayoshi, K., Ito, D. and Iwata, T., 2011. View Contact and Illuminance Distribution Provided by Blind Control for Glare-free Daylit Environment, Proc. of 27<sup>th</sup> CIE session, Vol.1, 747-750.
- Osterhaus W., 2008. Analysis of luminance histograms for the assessment of discomfort glare in daylit offices, Proc. of Balkan Light, 155-164.
- Sugano, S., Nakamura, Y., 2011. Generation of discomfort glare image using wavelet transform, Proc. of 27<sup>th</sup> Session of CIE, Vol.1, 286-293.
- Roh, H. and Udagawa, M., 2002. Comparison of air conditioning load among Tokyo and five European cities, *J. of Architectural Planning and Environmental Engineering*, Architectural Institute of Japan, No. 551, 45-52.
- Tuaycharoen, N., and Tregenza, P.R., 2005. Discomfort glare from interesting images, *J. of Lighting Research and Technology*, Vol. 37, No. 4, 329-341.
- Veitch, J. Charles, K., Kelly, Farley K. and Newsham, G. 2007 A model of satisfaction with open-plan office conditions: COPE field findings. *J. of Environmental Psychology*, Vol. 27, No. 3, 177-189.
- Wienold, J. and Christoffersen, J., 2006. Evaluation methods and development of a new glare prediction model for a daylight environment with the use of CCD cameras, *Energy and Buildings*, 38, 743-757.
- Wienold, J., 2009. Dynamic daylight glare evaluation, Proc. of Eleventh International IBPSA Conference, Building Simulation 2009, 944-951.
- Yun, G.Y., Shin, J. Y, Kim J. T., 2010. Influence of window views on the subjective evaluation of discomfort glare, 3rd International Symposium on Sustainable Healthy Buildings.